www.czasopisma.pan.pl PAN POLSKA AKADEMIA NAUK www.journals.pan.pl

PAN ARCHIVES OF ACOUSTICS
Vol. **43**, No. 1, pp. 83–92 (2018)

DOI: 10.24425/118083

Numerical Study of Acoustic-Structure Interaction of Selected Helicoidal Resonator with Flexible Helicoidal Profile

Wojciech ŁAPKA

Division of Vibroacoustics and Biodynamics of Systems
Institute of Applied Mechanics
Poznań University of Technology
Jana Pawła II 24, 61-139 Poznań, Poland; e-mail: wojciech.lapka@put.poznan.pl

(*received June 25, 2017; accepted August 28, 2017*)

The paper presents the results of numerical studies of acoustic-structure interaction of selected helicoidal resonator with helicoidal profile made of an elastic material. Considered a well-recognized acoustic system for one representative type of acoustic helicoidal resonator with two resonant frequencies that correspond to previous studies of the author. Due to the large range of flexible materials to study, this work focuses on the change of material density, Poisson's ratio and Young's modulus as the basic parameters describing the properties of elastic materials. The results indicate a significant interaction between the acoustic attenuation performance of helicoidal resonator and elasticity of the helicoidal profile. These interactions are most evident in the frequency range in which the helicoidal resonator is revealed to be effective acoustic damper.

Keywords: helicoidal resonator; acoustic-structure interaction; ducts and mufflers; numerical simulation; elastic materials.

1. Introduction

The paper presents the results of numerical studies of acoustic-structure interaction of selected helicoidal resonator with helicoidal profile made of an elastic material. Considered a well-recognized acoustic system (Łapka, 2007; 2009a; 2009b; 2010; 2012a; 2012b; 2012c) for one representative type of acoustic helicoidal resonator with two resonant frequencies that corresponds to previous studies of the author (Łapka, 2010; 2012b; Łapka, Cempel, 2008; 2011). Due to the large range of flexible materials to study, this work focuses on the change of material density, Poisson's ratio and Young's modulus as the basic parameters describing the properties of elastic materials. The results indicate a significant interaction between the acoustic attenuation performance of helicoidal resonator and elasticity of the helicoidal profile. These interactions are most evident in the frequency range in which the helicoidal resonator is revealed to be effective acoustic damper.

The numerical method to compute acoustic-structure interaction is so called "elastoacoustic problem" (Bermudez *et al.*, 2008). In this work we studied the determination of the transmission loss and displacement of an elastic structure of helicoidal profile in contact with a compressible fluid – air inside straight cylindrical duct. Comsol software with Acoustic Module and Material Library was used. Helicoidal profile was placed on perfectly hard mandrel, as interaction between fluid and structure could exist only between helicoidal profile and air.

Undertaken research was carried out to check the influence of helicoidal profile material properties on acoustic attenuation performance of helicoidal resonator. In order to obtain desired effect of acoustic-structure interaction, the material was set up as a rubber in first approach, but by the use of properties of different materials which were loaded directly from Material Library in Comsol software and change of the basic values of Young modulus – E in MPa, Poisson's ratio ν and density ρ in kg/m^3, many other materials were considered, for example: acrylic plastic, gold, silver, polysilicone, aluminum, titanium, high strength alloy steel, etc. On this base it is possible to conclude what the influence of different elastic properties applied as a material of helicoidal profile on the acoustic attenuation performance of helicoidal resonator is.

2. Description of investigated model

In correspondence with earlier research of acoustic properties of helicoidal resonators the considered geometrical relations of helicoidal resonator are the same as in previous example studies by Łapka (2009a; 2009b) and Łapka, Cempel (2007; 2008; 2011). Also, the ratio of the helicoidal skip s to cylindrical duct diameter d, $s/d = 1.976$ and the number of helicoidal turns $n = 0.671$, thickness of helicoidal profile $g = 3$ mm, the diameter of cylindrical duct $d = 125$ mm, and the diameter of mandrel $d_m = 30$ mm. In Fig. 1 the front and side views of investigated model of two resonant helicoidal resonators are presented. Figure 2 presents the view on investigated acoustic system with straight 3 m long cylindrical duct with helicoidal resonator inside.

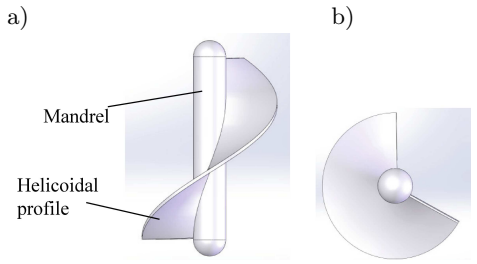

Fig. 1. Investigated model of two resonant helicoidal resonators with ratio $s/d = 1.976$, $n = 0.671$: a) side view, b) front view.

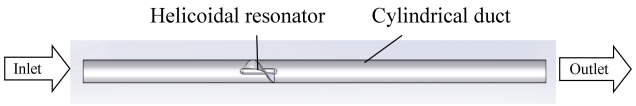

Fig. 2. Investigated acoustic system with helicoidal resonator inside straight 3 m long cylindrical duct.

For all cases considered in this work the temperature was set up to 20°C, it is 293.15 K, what can be designated as a room temperature.

3. Description of acoustic-structure interaction branch

The acoustic-structure interaction branch gives the possibility to simulate numerically in three dimensions (3D) a multiphysics phenomenon, as described in Comsol Multiphysics Users Guides (2010a; 2010b), where the acoustic pressure causes an air load on the solid domain, and the structural acceleration affects the air domain as a normal acceleration through the air-solid boundary. In this work he interface of acoustic-solid interaction in frequency domain was used, and it combines pressure acoustics, frequency domain and solid mechanics. Modelling acoustic problem in Comsol software (Comsol, 2010a; 2010b) in the frequency domain, means solving the Helmholtz equation. In this case only one time scale exists and it is set by the frequency $T = 1/f$, where T [s] means the time period and f [Hz] is the frequency.

3.1. Boundary conditions

The boundary conditions in acoustic-structure interaction define the nature of the boundaries in computational domain. Also we used a sound hard wall as the real physical obstacle – cylindrical duct walls and mandrel (Fig. 3), and artificial boundary condition as plane wave radiation at the inlet and outlet surfaces of duct (Fig. 4), used to simulate an open boundary where no sound is reflected. Also by the use of this boundary condition there is no need to simulate very

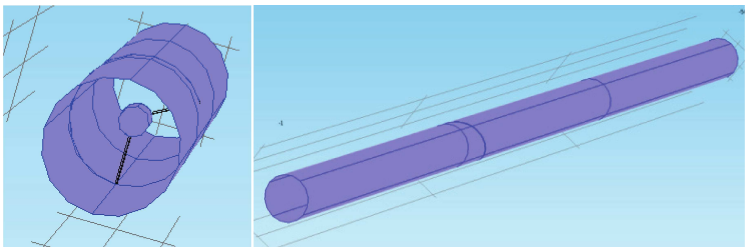

Fig. 3. Sound hard boundary condition (blue colour) on cylindrical duct and mandrel walls.

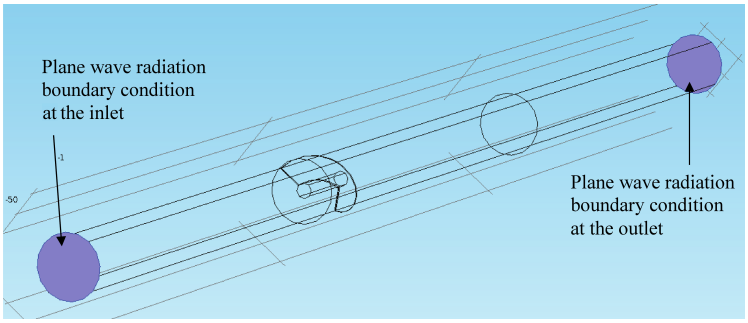

Fig. 4. Plane wave radiation boundary conditions (blue colour) on cylindrical duct inlet and outlet surfaces.

long pipe to obtain no reflections from the open end. Initial acoustic pressure at the inlet boundary was set as $p = 1$ Pa.

Free boundary condition means that there are no constraints and no loadings acting on the boundary. This boundary condition was set on helicoidal profile boundaries between mandrel and cylindrical duct walls, as it is presented in Fig. 5.

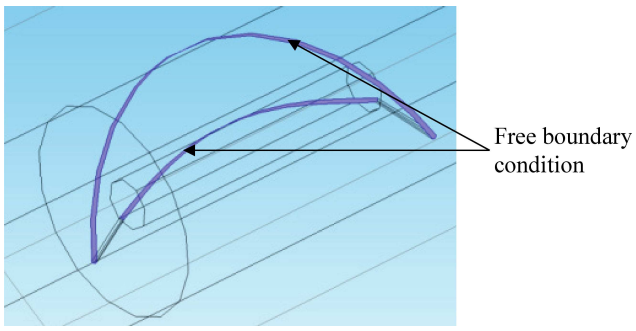

Fig. 5. Free boundary conditions (blue colour) at helicoidal profile boundaries between mandrel and cylindrical duct walls.

The characteristic and very important is acoustic-structure boundary condition between the air and the solid. This boundary condition includes the interaction between pressure load (force per unit area) on the boundaries where the air interacts with the elastic helicoidal profile and structural acceleration acting on those boundaries (Fig. 6). The latter makes the normal acceleration for the acoustic pressure on the boundary equal to the acceleration based on the second derivatives of the structural displacements with respect to time.

For rubber like materials, the solid model of helicoidal profile was set as isotropic linear elastic, temperature $T = 293.15$ K, absolute pressure $p_A = 1$ atm. As it was written before, the most important parameters of elastic materials as density, Young's modulus and Poisson's ratio were changed for each case. Parameters of the air were set as follows: density of air $\rho_A = 1.204$ kg/m^3, temperature of air $T_A = 293.15$ K, also speed of sound in air $c_s = 343$ m/s.

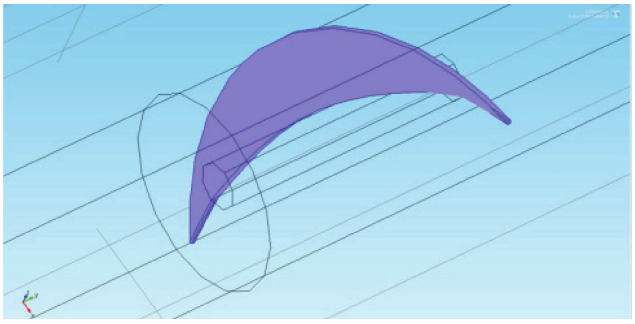

Fig. 6. Acoustic structure boundary conditions (blue colour) at the helicoidal profile surfaces between air and elastic material.

3.2. Mesh properties

Three dimensional mesh was generated in sequence type physics-controlled mesh with extra fine element size. Investigated model of cylindrical duct with helicoidal resonator inside after meshing is presented in Fig. 3. Table 1 presents types of mesh elements and statistics for entire geometry as shown in Fig. 7.

Table 1. Types of mesh elements and statistics for entire geometry.

No.	Description	Value
1.	Tetrahedral elements	100 091
2.	Triangular elements	15 984
3.	Edge elements	1403
4.	Vertex elements	52
5.	Minimum element quality	0.005704
6.	Average element quality	0.7332
7.	Element volume ratio	6.303e–7
8.	Mesh volume	0.0363 m^3
9.	Maximum growth rate	4.139
10.	Average growth rate	1.763
11.	Number of degrees of freedom	175 072

In this work the mesh, as presented above, has satisfied the rule in the frequency domain of five finite elements per highest considered frequency wave length.

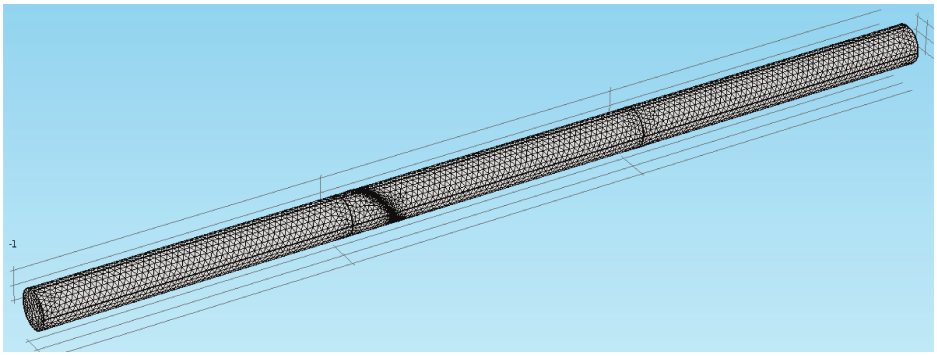

Fig. 7. Investigated straight 3 m long cylindrical duct with helicoidal resonator inside.

3.3. Acoustic attenuation performance

Transmission loss, TL [dB], was considered as an acoustic attenuation performance parameter in this work. It is commonly used parameter in the frequency domain and it describes what has been called "the muffler proper" (Munjal, 1987; Ver, Beranek, 2006). Also there is the difference between the incident sound power and outgoing sound power of the acoustic filter-cylindrical duct with helicoidal resonator in this work. It is independent on the source and outlet of the pipe – anechoic inlet and outlet. In numerical investigations one takes into account the integrated sound intensity at the inlet and outlet surfaces where the specific plane wave radiation is applied, as described above, and the difference between them is calculated for every considered frequency.

In this work the investigated frequency range was analyzed from 1100 Hz to 1450 Hz with the step of 1 Hz. It is the characteristic frequency range of induced sound attenuation by the phenomenon of acoustic resonance of helicoidal resonator.

4. Results

This chapter presents the results of numerical calculation of an acoustic-structure interactions and transmission loss characteristics for investigated cylindrical duct with helicoidal resonator. The following properties of helicoidal profile material were changed: density ρ [kg/m^3], Young's modulus E [MPa] and dimensionless Poisson's ratio ν.

Due to many possibilities of applying different materials properties, hard and dense metals were selected in Sec. 1, few examples of non-metals elastic materials in Sec. 2 and only rubber in Sec. 3.

4.1. Metals

In order to make a comparison between hard and elastic materials we have started with some examples of hard and dense materials – metals. In Fig. 4 we present numerically calculated transmission loss characteristics of investigated type of helicoidal resonator, $n = 0.671$, with helicoidal profile made from nominally hard material like aluminum, titanium, gold, silver, high strength alloy steel. The properties of these materials are presented in Table 2.

Table 2. Selected properties of investigated metals.

Material	Density ρ [kg/m^3]	Young's modulus E [MPa]	Poisson's ratio ν
Silver	10 490	81 137	0.37
Gold	19 282	75 765	0.44
High strength alloy steel	7850	200 000	0.33
Aluminum	2700	70 000	0.33
Titanium beta 21S	4940	105 000	0.33

As it can be observed in Fig. 8, the transmission loss characteristics of helicoidal resonator with helicoidal profile made from example metals do not change significantly. The most evident difference one can

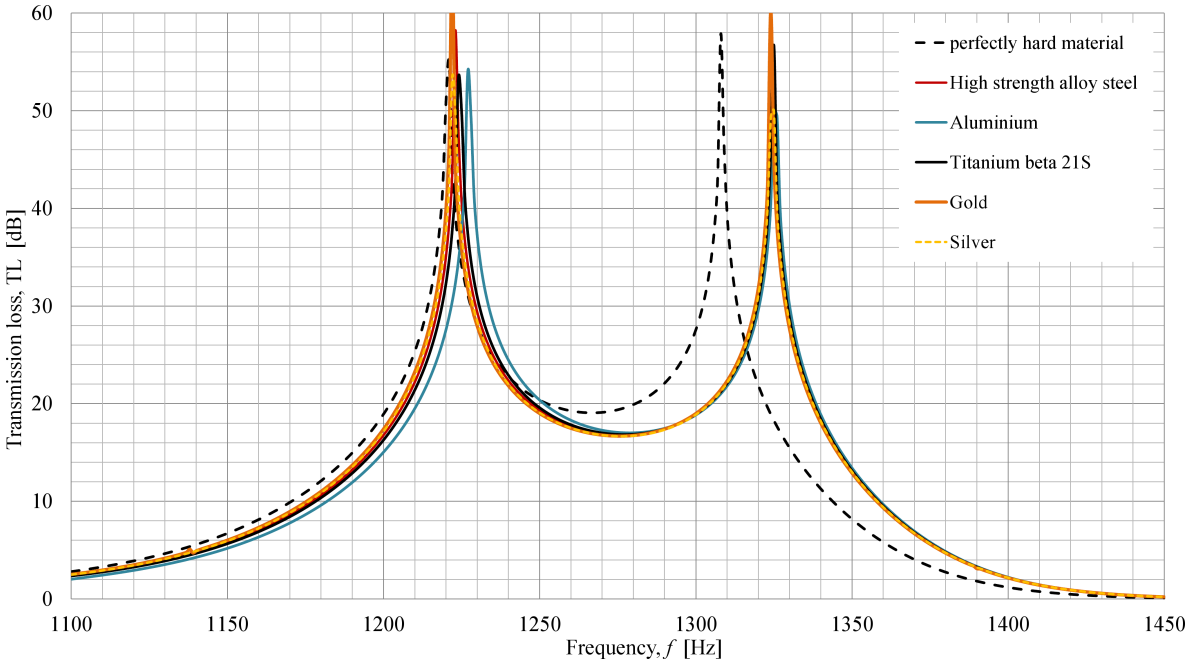

Fig. 8. Transmission loss characteristics of investigated helicoidal resonator with helicoidal profile made from selected metals.

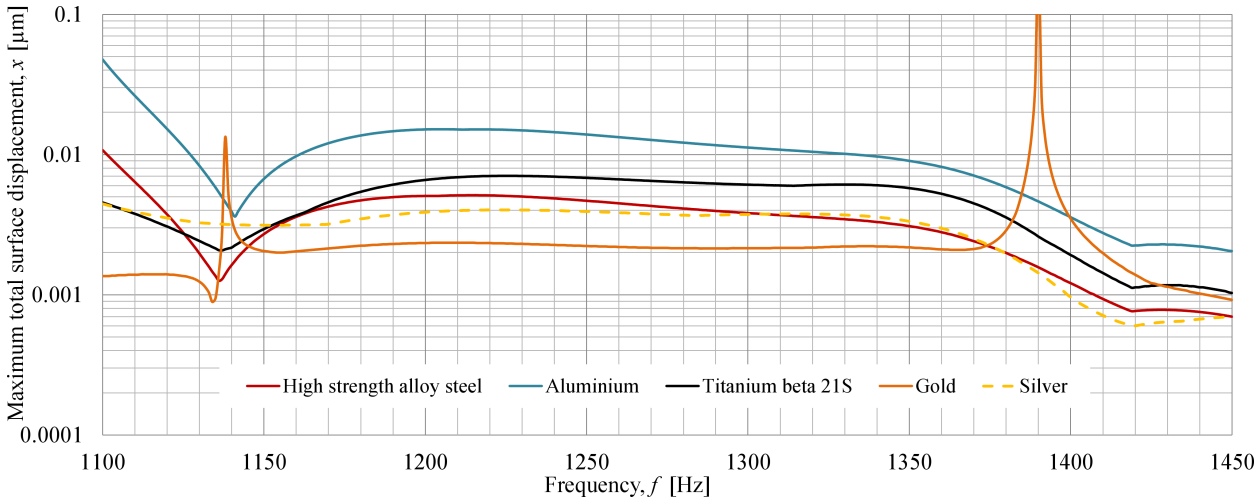

Fig. 9. Maximum total surface displacement characteristics for investigated helicoidal resonator with helicoidal profile made from selected metallic materials.

observe between ideally hard material and other hard metallic materials for the second resonance frequency of investigated helicoidal resonator. Perfectly hard and reflective material means that basically there is an empty space without air, and in reality probably every kind of material in some part could transmit the sound through 3 mm thick helicoidal profile. Also perfect reflection in this case can't exist in practice. This is an important observation due to possible design of helicoidal resonators for real ducted systems, where each components could be made of metals or other hard materials.

The maximum total surface displacement characteristics for helicoidal profile made from metals are presented in Fig. 9, and one can observe no significant changes of them.

4.2. Non-metals

In this subsection we discuss selected non-metallic materials properties (Brandrup *et al.*, 1999) that are presented in Table 3 – excluding rubber, which is described in Subsec. 4.3. Also we present selected materials from wide range of Young's modulus from 2000 MPa to 170 000 MPa and quite wide range of Poisson's ratio from 0.17 to 0.4, but not so wide density from 1150 kg/m^3 to 2329 kg/m^3.

Table 3. Selected properties of investigated non-metallic materials (Brandrup *et al.*, 1999).

Material	Density ρ [kg/m^3]	Young's modulus E [MPa]	Poisson's ratio ν
Polysilicone	2320	169 000	0.22
Silica Glass	2203	73 100	0.17
Silicone	2329	170 000	0.28
Acrylic plastic	1190	3200	0.35
Nylon	1150	2000	0.4
Rubber	900–2000	10–100	0.48–0.5

As it can be observed in Table 3 the rubber properties are more varied than others due to much smaller Young's modulus and larger Poisson's ratio. This is the reason why there is a part of calculations destined only for rubber in subsection 4.3 with different density and Young's modulus, as well as significant change of Poisson's ratio.

Figure 10 shows transmission loss characteristics for helicoidal profile made from materials with properties as in Table 3.

As it can be observed in Fig. 6 the transmission loss characteristics differ from each other. The important observation is that the elastic properties of investigated materials mainly reflect in the biggest difference in Young's modulus, known as elastic modulus. Figure 11 also presents maximum total surface displacement characteristics of helicoidal profile for non-metallic materials.

Acrylic plastic has the biggest surface displacement between frequencies 1140 Hz and 1150 Hz that is nearly 6 µm. Silicone and polysilicon have the same displacement.

4.3. Rubber

In this subsection rubber properties applied to helicoidal profile are considered. The range of density ρ and Young's modulus E, as well as Poisson's ratio ν, give the opportunity to divide the research into three cases:

1) constant E, constant ν, different ρ;
2) constant E, different ν, constant ρ;
3) different E, constant ν, constant ρ.

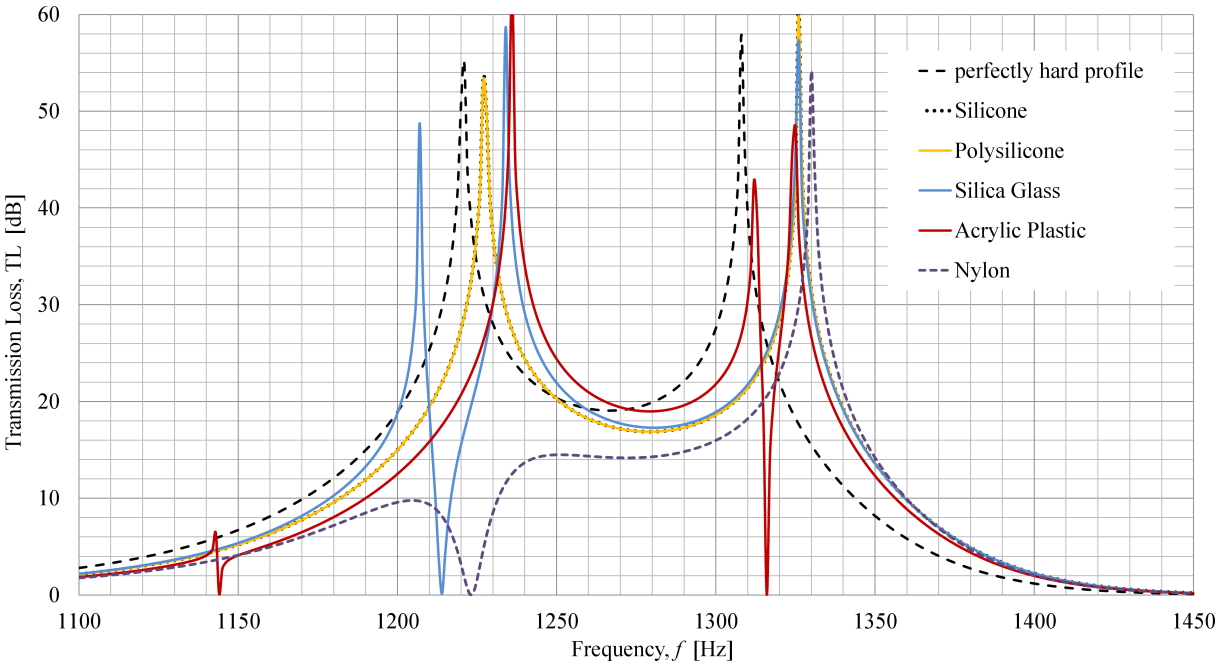

Fig. 10. Transmission loss characteristics of investigated helicoidal resonator with helicoidal profile made from selected non-metallic materials.

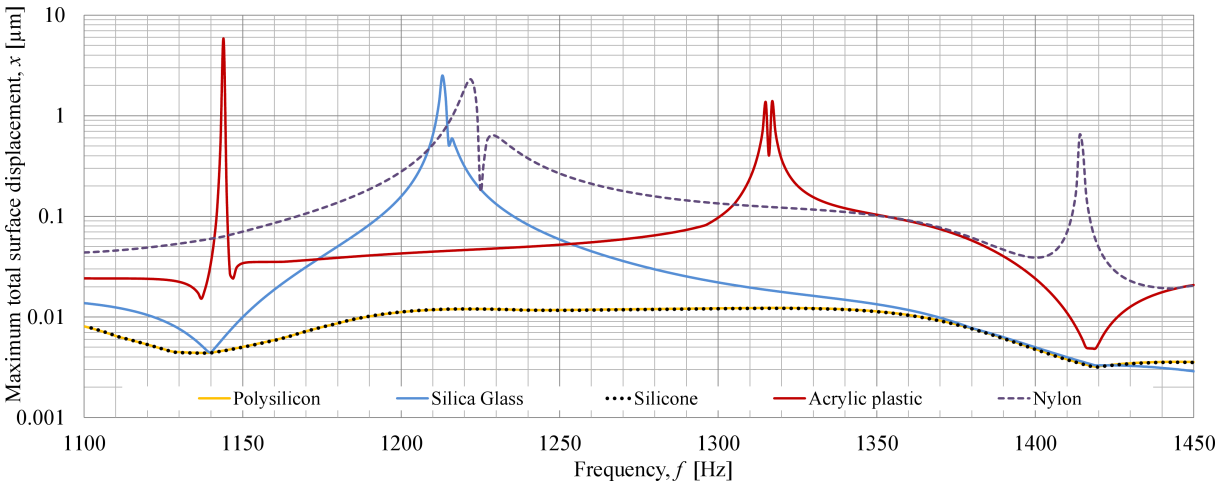

Fig. 11. Maximum total surface displacement characteristics for investigated helicoidal resonator with helicoidal profile made from selected non-metallic materials.

Figure 12 presents TL characteristics while Fig. 13 the maximum total surface displacement characteristics for a first case.

TL characteristics for three considered densities are close to each other in the frequency range and characteristic resonances, as well as in levels of attenuation. Global conclusion could be that the more dense is the material the more similarities of the TL characteristic to perfectly hard material are observed. But there are some visible rapid changes of TL in some frequencies, which are connected with peaks in maximum total surface displacement characteristics. And they are not regular. Also for density $\rho = 1000$ kg/m^3 there is a visible peak of TL near 1170 Hz, before first characteristic resonance of helicoidal resonator, which has an analogous displacement peak of about 3 μm. There is a second strong change in TL near the second characteristic resonance of helicoidal resonator and similarly nearby there are visible two displacement peaks of about 3 μm. There are also visible some smaller changes, which can be neglected due to small influence on TL, but the highest peak of displacement near 1275 Hz has about 2 μm.

For the density $\rho = 1500$ kg/m^3 there are smaller changes in TL near 1160 Hz and 1260 Hz and one strong change of TL near 1240 Hz just over the first characteristic resonance of helicoidal resonator. Therefore, it is interesting that there are visible three biggest

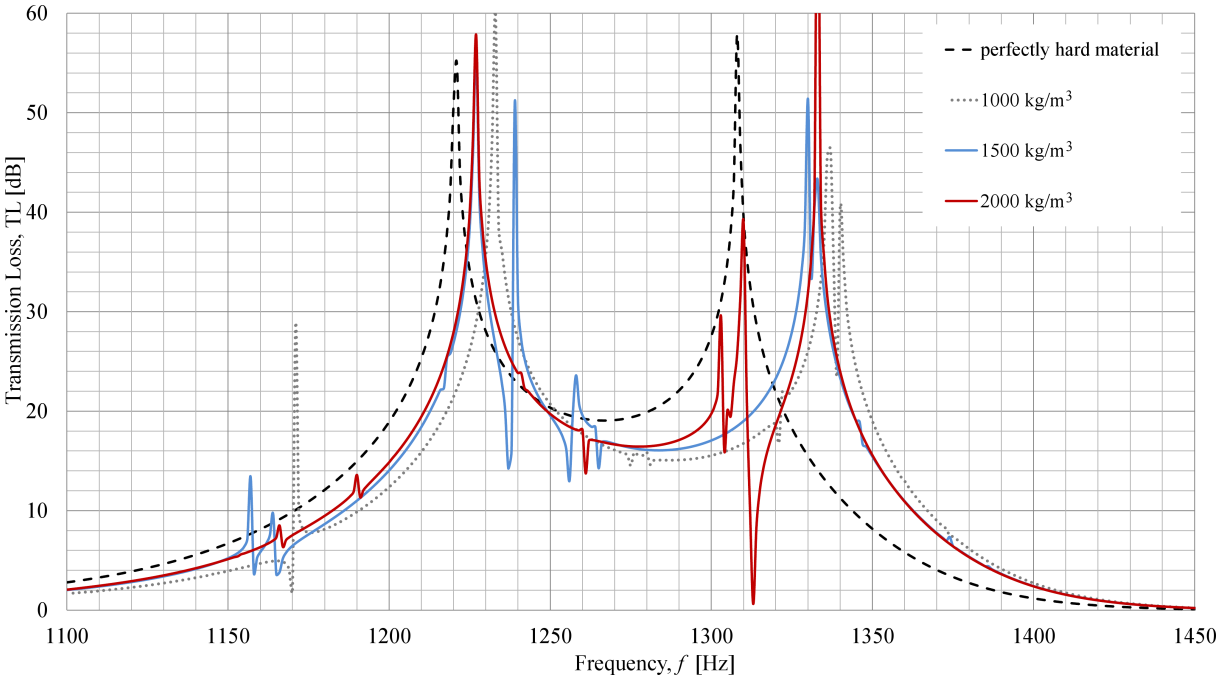

Fig. 12. Transmission loss characteristics for helicoidal profile made from rubber with different ρ [kg/m^3] and constant $E = 100$ MPa and $\nu = 0.49$.

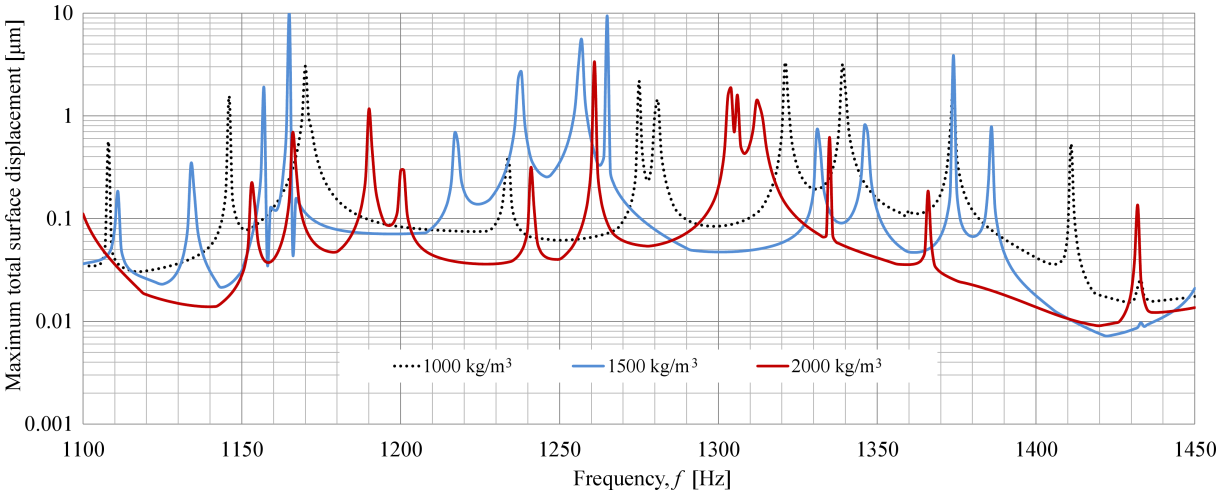

Fig. 13. Maximum total surface displacement characteristics for helicoidal profile made from rubber with different ρ [kg/m^3], constant $E = 100$ MPa and $\nu = 0.49$.

displacement peaks from about 4 μm to 10 μm, but the TL characteristic does not change significantly.

The TL characteristic for the density $\rho = 2000$ kg/m^3 has one strong change near 1310 Hz and there is a helicoidal profile displacement of almost 2 μm in frequency range between 1300–1320 Hz just before the second characteristic resonance frequency of investigated helicoidal resonator.

Figure 14 presents TL characteristics and Fig. 15 presents maximum total surface displacement characteristics for second case, where constant Young's modulus $E = 10$ MPa, constant $\rho = 1000$ kg/m^3, and different Poisson's ratio ν are considered. Here, visible a large change in TL characteristics for about 1210 Hz is visible, and similarly to first case there is frequency range between 1200–1220 Hz with a helicoidal profile displacement of almost 2 μm for every investigated Poisson's ratio, but the highest peak is obtained for $\nu = 0.49987$.

Figure 16 presents TL characteristics and Fig. 17 presents maximum total surface displacement characteristics for third case, where constant Poisson's ratio $\nu = 0.49$, constant density $\rho = 1000$ kg/m^3 and different Young's modulus E are considered. Here, one can observe the highest peak in all considered cases in this paper. It occurs for helicoidal profile made from

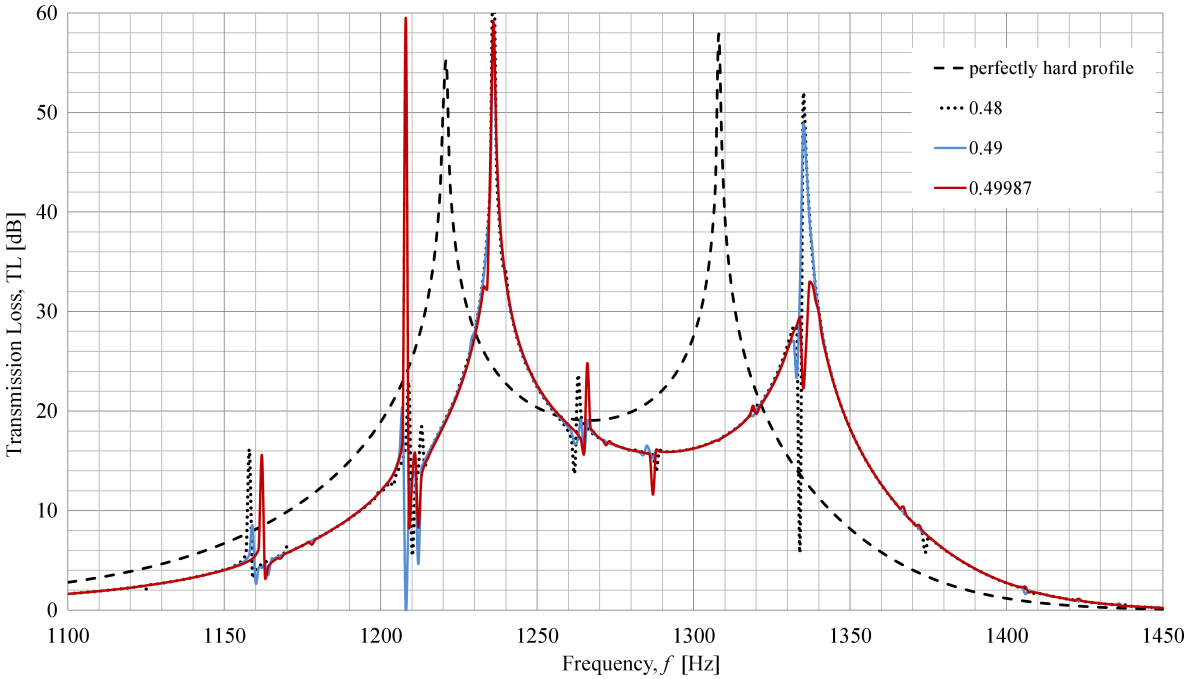

Fig. 14. Transmission loss characteristics for helicoidal profile made from rubber with different ν, constant $E = 10$ MPa and $\rho = 1000$ kg/m^3.

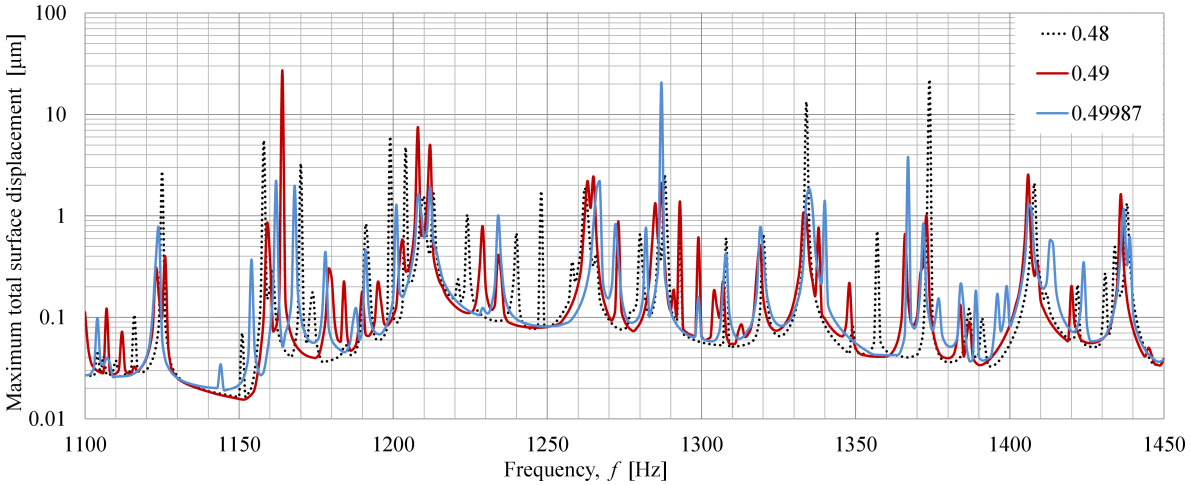

Fig. 15. Maximum total surface displacement characteristics for helicoidal profile made from rubber with different ν, constant $E = 10$ MPa and $\rho = 1000$ kg/m^3.

rubber with Young's modulus $E = 0.05$ GPa and the maximum total surface displacement has about 50 μm in the frequency about $f = 1264$ Hz. The transmission loss for that frequency is lower (TL equals about 6 dB) than expected for non-elastic materials.

5. Conclusions

In this work we have considered the acoustic-structure numerical simulations for selected two resonant helicoidal resonator of ratio s/d= 1.976 and number of helicoidal turns n= 0.671 with helicoidal profile made from different materials. Properties of metals and non-metals, especially rubber, were considered. Due to focusing on possible influence of elasticity of helicoidal profile on the acoustic attenuation performance of helicoidal resonator, three main parameters were changed: material density, Poisson's ratio and Young's modulus known as elasticity modulus. The results show that it seems to be a proper assumption that the most evident of the material properties could be the density, because of the biggest change of transmission loss characteristics. Thus, first of all this parameter should be taken into account when designing helicoidal resonators for real acoustic systems.

Global conclusion for considered cases of flexible profile of the helicoidal resonator tends to formulation

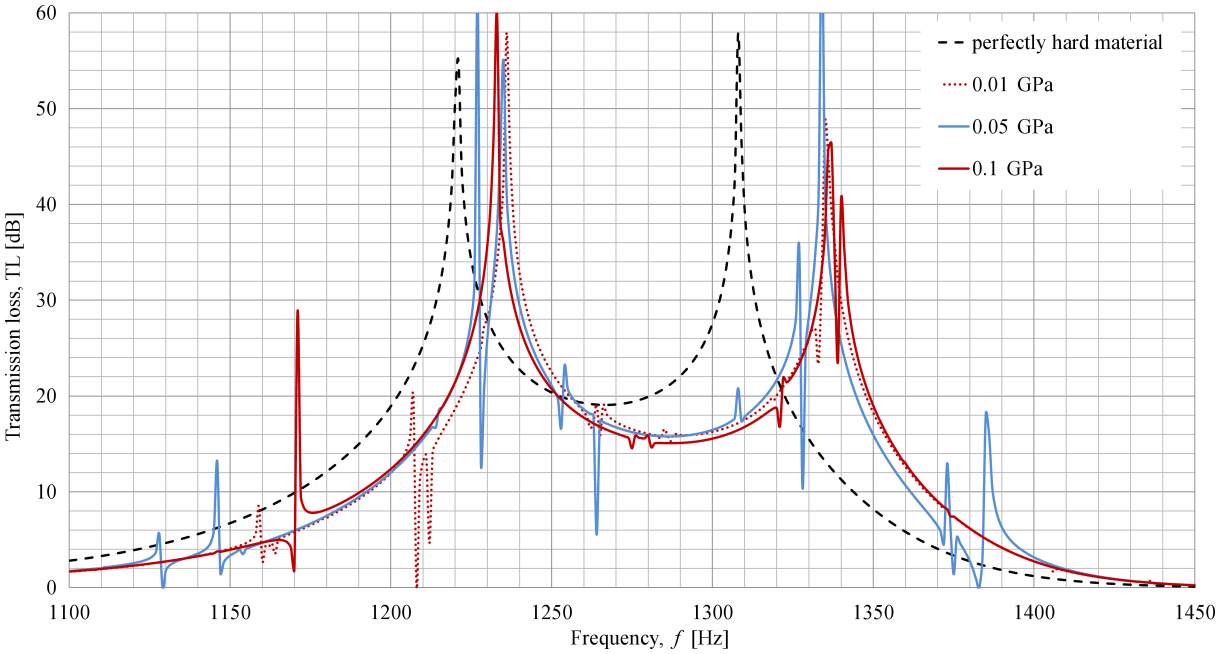

Fig. 16. TL characteristics for helicoidal resonator with profile made from rubber with constant $\nu = 0.49$, constant $\rho = 1000$ kg/m^3, and different Young's modulus E in GPa.

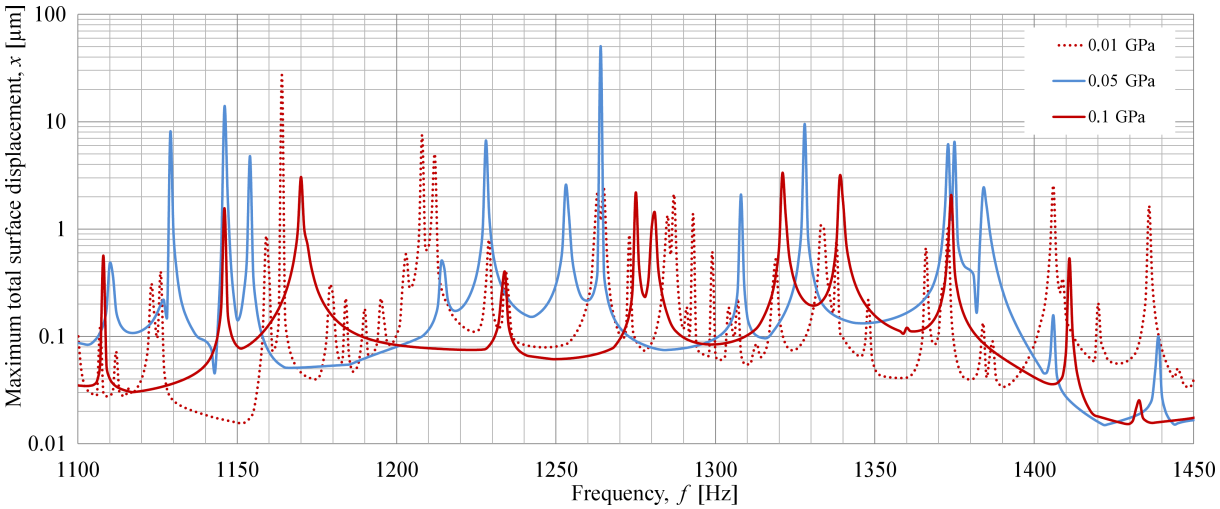

Fig. 17. TL characteristics for helicoidal resonator with profile made from rubber with constant $\nu = 0.49$, constant $\rho = 1000$ kg/m^3, and different Young's modulus E in GPa.

that applying the elastic material could decrease the sound attenuation induced by its acoustic resonance. Maybe one can find some specific range of elastic materials and their properties that can give some added value to improve the helicoidal resonators acoustic attenuation performance, but this research work does not confirm these assumptions.

Acknowledgments

This work was supported by grants of the Ministry of Science and Higher Education in Poland (NN502455739 and 02/21/DSPB/3494/2017). The simulations were carried out at the Poznan University of Technology in Institute of Applied Mechanics.

References

1. Bermudez A., Gamallo P., Hervella-Nieto L., Rodriguez R., Santamarina D. (2008) *Fluid-Structure Acoustic Interaction*, [in:] *Computational Acoustics of Noise Propagation in Fluids, Part III: FEM related problems*, S. Marburg, B. Nolte [Eds.], Ch. 9, pp. 253–306.

2. Brandrup J., Immergut E.H., Grulke E.A., Abe A., Bloch D.R. (1999), *Polymer handbook*, 4th Ed., John Wiley & Sons, Inc.

3. Comsol Multiphysics (2010a), *Users Guide – Modeling Guide and Model Library, Documentation Set*, COMSOL AB, Stokholm, Sweden.

4. Comsol Multiphysics (2010b), *Users Guide, Acoustic Module Documentation Set*, COMSOL AB, Stokholm, Sweden.

5. Łapka W. (2007), *Acoustic attenuation performance of a round silencer with the spiral duct at the inlet*, Archives of Acoustics, **32**, 247–252.

6. Łapka W. (2009a), *Acoustical properties of helicoid as an element of silencers*, Doctoral work, Faculty of Mechanical Engineering and Management, Poznań University of Technology, Poland.

7. Łapka W. (2009b), *Insertion loss of spiral ducts – measurements and computations*, Archives of Acoustics, **34**, 4, 537–545.

8. Łapka W. (2010), *Helicoidal resonator*, Proceedings of the 39th International Congress and Exposition on Noise Control Engineering INTER-NOISE 2010, 9 pages on CD-ROM, Lisbon, Portugal.

9. Łapka W. (2012a), *Comparison of numerically calculated pressure drop for selected helicoidal resonators*, Proceedings of the 59th Open Seminar on Acoustics, OSA2012, Boszkowo-Poznań, Poland, pp. 145–148.

10. Łapka W. (2012b), *Multi resonant helicoidal resonator for passive noise control in ducted systems*, [in:] Silva Gomes J.F., Vaz M.A.P. [Eds.], Proc. of 15th International Conference on Experimental Mechanics, Paper ref.: 2682, Porto, Portugal.

11. Łapka W. (2012c), *Numerical aeroacoustic research of transmission loss characteristics change of selected helicoidal resonators due to different air flow velocities*, Vibrations in Physical Systems, **25**, 267–272.

12. Łapka W., Cempel C. (2007), *Noise reduction of spiral ducts*, International Journal of Occupational Safety and Ergonomics, **13**, 4, 419–426.

13. Łapka W., Cempel C. (2008), *Computational and experimental investigations of a sound pressure level distribution at the outlet of the spiral duct*, Archives of Acoustics, **33**, 4 Supplement, 65–70.

14. Łapka W., Cempel C. (2011), *Acoustic short helicoidal resonator-computational and experimental investigations*, Proceedings of the 58th Open Seminar on Acoustics, OSA 2011, Gdańsk-Jurata, Poland, pp. 9–16.

15. Munjal M.L. (1987), *Acoustics of Ducts and Mufflers with Application to Exhaust and Ventilation System Design*, John Wiley & Sons, Inc., Calgary, Canada.

16. Ver I.L., Beranek L.L. (2006), *Noise and vibration control engineering*, 2nd Ed., John Wiley & Sons, Inc., Hoboken, New Jersey, USA.